# STATISTICAL ASSESSMENT OF NATURAL FREQUENCY VALUES OBTAINED FROM NUMERICAL ANALYSES IN THE TAPERED COMPOSITE LAMINATED BEAMS

by

***Ismail OVALI****

Department of Mechanical Engineering, Faculty of Technology University of Pamukkale, Denizli, Turkey

Original scientific paper
https://doi.org/10.2298/TSCI2304241O

*In the last years, the glass/epoxy laminated composites which are a combination of glass reinforcement and epoxy matrix are widely used in the field of automotive and aerospace due to their strength/weight ratio. The proposed study statistically evaluates the natural frequency data obtained by the numerical analysis of glass reinforced epoxy matrix beams with Taguchi method. Accordingly, numerical analyzes were performed based on L27 orthogonal array at different levels of tapered angle (0, 0.25, and 0.5), fiber orientation angle (30°, 600°, and 900°), and a/l ratio (delamination ratio) (0, 0.25, and 0.5). The obtained results were evaluated with analysis of variance (ANOVA), regression analysis, main effects, and interactions plots. Lastly, it was observed that the tapered angle changes directly with the natural frequency and inversely with a/l delamination rate, and there is a dramatic increase in the natural frequency at the 30° angle. With regression analysis, the effects of main, interaction, and squares of factors on natural frequency are predicted with a coefficient of determination of 95.63%. Finally, the optimum natural frequency is obtained at third level of the tapered angle (A = 0,5), the first level of angle (B = 30°) and a/l ratio (C = 0) as 40.091 Hz.*

Key words**:** *glass-epoxy laminated composite beam, vibration, ANOVA, finite element analysis*

## Introduction

Compared to metal materials, composite materials have a wide range of uses in aircraft, ships, automotive, and defense industries with their high strength to weight ratio, high rigidity, fatigue resistance, and long service life, Guo *et al.* [1], Zakaria *et al.* [2], Yalcin and Ergene [3], Zhang *et al.* [4], and Wang [5]. However, these materials also tend to damage and defect, which significantly reduces their structural integrity. The damages due to the weak strength of the laminated composite structure between the layers usually lead to interlayer fractures, in other words, the formation of the discontinuity zone (delamination). Delaminations can be caused by either a faulty manufacturing process such as incomplete wetting (under-applying resins) and the formation of interlayer air pockets, or a foreign body impact. It is known that such delamination damage causes a decrease in the strength and stiffness of the laminates. As a result, delaminations cause a change in vibration characteristics, Imran *et al.* [6]. Delaminated layers often exhibit new vibrational modes and frequencies depending on the

* Author's, e-mail: iovali@pau.edu.tr

number, location, and size of the delamination. In particular, delaminations reduce the natural frequency, which causes resonance leading to damage to the structure when this low frequency is equal to the operating frequency. Therefore, it is essential to predict changes in frequency as well as mode shapes in a dynamic environment. Below, some studies in this field are evaluated.

Wang *et al.* [7] performed a study about the vibration characteristics of sandwich panels with a hierarchical composite honeycomb sandwich core. An orthotropic constitutive model of the hierarchical composite honeycomb sandwich core was used to propose an equivalent model (2-D model). The 2-D and 3-D finite element models as well as modal tests were used to predict the natural frequencies and mode shapes of the sandwich panels. Hosseini *et al.* [8] conducted experimental research using ultrasonic guided waves for damage detection in honeycomb cellular structures. They supported their experimental studies with numerical approaches using the finite element method. Sayyad and Ghugal [9] studied sandwich composite structures with lamina structure, which they showed as usable in many structures, including mechanical and aerospace engineering. In their study, they discussed free vibration analysis, theories based on sandwich layers, zig-zag theories, and structures subjected to isotropic buckling. Ramtekkar [10] used a finite element model for the 2-D plane stress state to analyze the free vibrations of delaminated laminated beams. The mode shapes and frequencies of the delaminated beams were calculated by presenting the contact-interface model and the unconstrained-interface model.

Alnefaie [11] developed a 3-D finite element model for the dynamic analysis of delaminated composite plates. The natural frequency and mode shapes of the plate were calculated for different delaminations. In his paper, the finite element model was conducted with ABAQUS software. Della and Shu [12] presented an analytical solution for the free vibration of a multi-delaminated beam under compression load. An analytical model was created by dividing the delaminated beam into seven interconnected Euler-Bernoulli beams. The delaminated beam with 14 layers was modeled as a free and constrained model. Zhang *et al.* [13] investigated the modal performance of honeycomb structures of micro-perforated sandwich beams. They used FEM and modal analysis techniques to find the vibration properties of the system. They proposed a dimensionless frequency parameter to determine the influence of the diameters of the micro-structures on the natural frequencies of the sandwich beams. As a result, they obtained that the frequency parameter of the sandwich panels decreased linearly with the increase in the ratio of the microstructure diameter. Wang *et al.* [14] investigated the vibration properties of composite honeycomb sandwich panels. They designed the sandwich model in orthotropic form, as both 2-D and 3-D, and observed the frequency values via the finite element method. They determined that the analyzes carried out in the FEM environment show good agreement with the experimental results. Atlihan *et al.* [15] showed that natural frequency values and buckling loads of the beam can be modified by changing the sequence angles of the beam without changing the weight or geometry of the laminated composite beam. They performed the vibration and buckling analyzes by assuming the laminated composite beam as the Euler-Bernoulli beam.

The proposed study, unlike other studies, statistically investigates the effects of tapered angle, orientation angle, and $a/l$ ratio factors on natural frequency. Accordingly, the optimum levels of these factors are determined, and the natural frequency performance of the system is modeled statistically.

## Material and method

In this study, finite element analyzes of glass reinforced epoxy matrix laminated composite beams with delamination were performed in the ANSYS APDL program [16]. Shell 99 element type, which provides vibration, layered structure, and composite material properties, which can be used for layered structural shell models, is preferred as an element type. Moreover, Shell 99 element type allows working with up to 250 layers and that is used in orthotropic materials with 6 DoF by rotation and translation in the *x*-, *y*-, and *z*-directions. In the study, the laminated composite beam with eight layers is modeled. The model has 1500 elements and 1661 nodes, and the mechanical properties of the beam used in the analysis are given in tab. 1.

**Table 1. Material properties and dimensions of the glass/epoxy laminated composite beam, Atlihan and Ergene [17]**

| Properties | Symbol | Values |
|---|---|---|
| Longitudinal elasticity modulus | $E_1$ [MPa] | 44150 |
| Transverse elasticity modulus | $E_2$ [MPa] | 12300 |
| Shear modulus | $G_{12}$ [MPa] | 4096 |
| Poisson's ratio | $\upsilon_{12}$ | 0.2 |
| Density | $\rho$ [kgm$^{-3}$] | 2026 |
| Length | $L$ [mm] | 200 |
| Height | $h$ [mm] | 3 |
| Width | $b$ [mm] | 20 |
| Delamination length | $a$ [mm] | 40 |

In figs. 1 and 2, the meshed state of the glass/epoxy laminated beam and the distribution of fiber angles of the eight-layer composite beam are given, respectively.

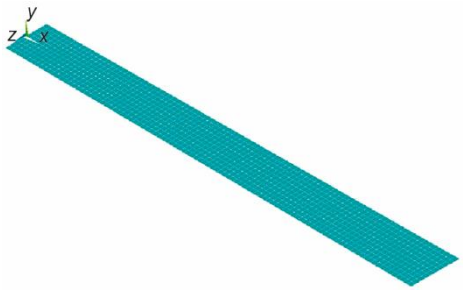


**Figure 1. Encastre fixed glass/epoxy laminated composite beam**

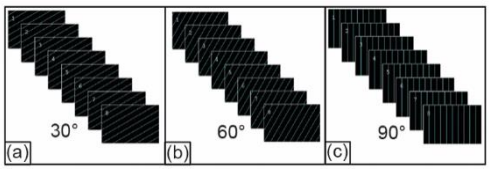


**Figure 2. Representation of fiber angles of laminated composite beam; (a) 30°, (b) 60°, and (c) 90°**

Initially, the composite beams are modeled in order to get an initial estimation of the undamped natural frequencies, $\omega_n$, and mode shape, $n$. This element is constituted by layers that are designated by numbers (LN – Layer number), increasing from the bottom to the top of the laminate; the last number quantifies the existent total number of layers in the laminate (NL

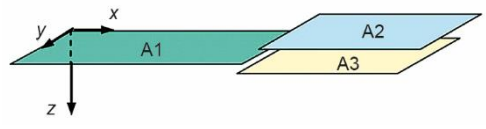


**Figure 3. Laminated composite beam with edge delamination**

– total number of layers). Thus, the model of the laminated composite beam is generated using eight layers. Table 1 gives the geometry and material properties of the laminated beams used. The boundary conditions have been applied on the nodes in the *y*-*z* plane, in which the origin of the axes is located. The DoF of all nodes about the *y*-*z* plane, which include displacements and rotations, are taken as zero. The dimensions of the beams in the *x*- and *y*-co-ordinates are $L$ = 200 and $b$ = 20 mm. Figure 3 shows the position of the edge delamination and laminated composite beams having edge delamination, which consist of three areas. In the beams with edge delamination, area A1 is glued with areas A2 and A3, but the interface of A2 and A3 is not glued. Glue is a command in the ANSYS software program that is applied only to cases in which the intersection between entities occurs at a boundary, and is satisfied connected at their intersection. The entities maintain their individuality, Atlihan and Ergene [17] and Callioglu [18].

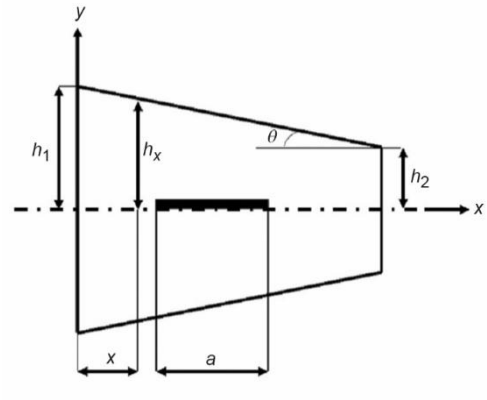


**Figure 4. The varies of the cross-section in a beam with delamination length *a*, [17]**

Since the beam has a variable cross-section, fig. 4, it is defined by function $f(x)$ with variable intercept, Callioglu [18], Ramalinggeswara and Ganesan [19], $\theta$ is tapered angle, $h_x$ is half thickness depending on $x$, $h_1$ is the maximum half thickness and $h_2$ is the minimum half thickness.

## Statistical assessment

In the presented study, the effects of important factors such as tapered angle, orientation angle, and *a*/*l* ratio and their interactions on natural frequency, $NF_n$, in laminated composite beams are evaluated with Taguchi method and regression analysis at 95% confidence interval. The proposed method can easily determine the effects of factors and interactions on the response and the optimum levels in a low number of experiments without the need for complex calculations. It also provides the opportunity to work with test plans of other experimental design methods. The factors used in the study and their levels are given in tab. 2.

**Table 2. Factors and their levels**

| Process parameters | Levels | | |
|---|---|---|---|
| | 1 | 2 | 3 |
| Tapered angle (A) | 0 | 0.25 | 0.5 |
| Orientation angle (B) [°] | 30 | 60 | 90 |
| *a*/*l* ratio (C) | 0 | 0.25 | 0.5 |

The choice of OA, which directly affects the number of experiments and the accuracy of the study, is determined based on the total DoF of the factors and interactions. The

DoF of the selected OA must be greater than or equal to the DoF of the system. The DoF of the experimental system is determined by adding the DoF of the factors and interactions, Shridhar [20], Unal and Dean [21], and Phillip [22]. The DoF of the relevant factor is determined as the number of levels belonging to that factor – 1. Accordingly, since there are three factors in our experiment, the DoF of the factors is 3 × 2 = 6. In the interactions, it is calculated by multiplying the DoF of the factors that create the interaction. Since there are 3 interactions in the system, their DoF is 3 × 4 = 12. In the light of these data, DoF of the system is calculated as 6 + 12 = 18. In the experiments, L27 OA, consisting of 13 columns and 27 rows with 26 DoF.

This array also constitutes the experimental design, and the 27 rows in the array represent the analyses in different combinations of factors. Process parameters are also assigned to the columns of the array. Figure 5 shows the assignment process obtained through the linear graph method. Thus, the first column in the OA is assigned to the tapered angle, the second one to the orientation angle, the fifth one to the *a*/*l* ratio, and the remaining columns are assigned to the interactions, Pinar [23], Pinar *et al.* [24], and Pinar and Firat [25].

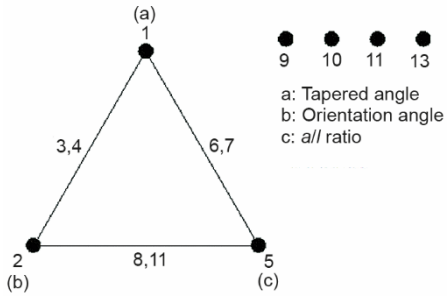


**Figure 5. Assignment of process parameters to the OA columns**

**Table 3. The ANOVA results**

| Source | DoF | *SS* | *V* | *F* | *P* |
|---|---|---|---|---|---|
| Tapered angle (A) | 2 | 1.054 | 0.527 | 12.26 | 0.31 |
| Orientation angle (B) | 2 | 233.887 | 116.944 | 2719.63 | 68.97 |
| The *a*/*l* ratio (C) | 2 | 67.911 | 33.955 | 789.65 | 20.03 |
| A × B | 4 | 0.028 | 0.007 | 0.16 | 0.01 |
| A × C | 4 | 35.164 | 8.791 | 204.44 | 10.37 |
| B × C | 4 | 0.741 | 0.185 | 4.30 | 0.22 |
| Error | 8 | 0.345 | 0.043 | | 0.10 |
| Total | 26 | 339.130 | | | 100 |

*SS* – sum of squares, *V* – variance, *P* – percent of contribution, $F_{0.05,2,8}$ = 4.46, $F_{0.05,4,8}$ =3.84

## Experimental results and statistical analysis

Analysis results ($Nf_c$ values in tab. 4) that conducted based on L27 OA, are evaluated at 95% confidence interval using MINITAB statistical software with ANOVA and regression analysis.

The ANOVA is a statistics-based tool that evaluates the significance of the factors and interactions of the experimental design on the quality characteristic at a specific confidence level, Pinar [23], Pinar *et al.* [24], and Pinar and Firat [25]. The ANOVA results of the analyzes are given in tab. 3. Significant process parameters in ANOVA are determined by the *F* value of the corresponding factor or interaction in the fifth column of the table. The *F* value of the relevant parameter is compared with the *F*-table value ($F_{0.05}$) at a 0.05 level

of significance. If the $F$ value is greater, the parameter is accepted as significant, Pinar and Firat [25]. The last column of the table expresses the percentage distribution of the process parameters on the natural frequency. In other words, it can also be called as significance ratio. In this manner, it is observed that all process parameters are significant, except for tapered angle-orientation angle interaction. In addition, orientation angle ($P$ = 68.97%) has the most significant effect on the $NF_n$, and it is followed by $a/l$ ratio (20.03%), tapered angle-$a/l$ ratio (10.37%), tapered angle (0.31%), orientation angle-$a/l$ ratio (0.22%) factors and interactions.

## Determination of optimum factor levels

Optimum levels are determined by taking into account ANOVA, main effect plots and interaction plots. According to the main effects plot, fig. 6, it is seen that the $NF_n$ correlates positively with tapered angle but negatively with $a/l$ ratio, and there is a dramatic increase in the $NF_n$ in the orientation angle of 30°. Due to the low slope of tapered angle and low percentage distribution of this factor in ANOVA, the 3rd level of the tapered angle can be taken for the maximization of the $NF_n$ according to both graphs when the interaction graph of A × C with a higher percentage distribution, fig. 7, is examined. Thus, the maximum $NF_n$ is obtained at the third level of the tapered angle ($A$ = 0.5), the first level of the fiber angle ($B$ = 30°) and the first level of the $a/l$ ratio ($C$ = 0) as 40.091 Hz (Analysis no. 19).

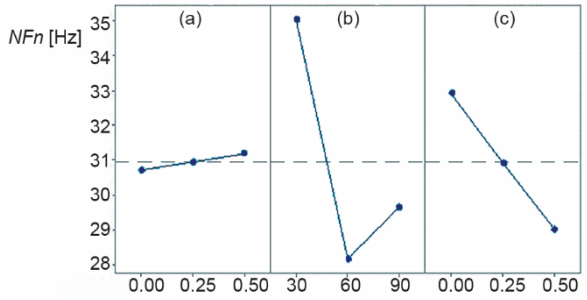


**Figure 6. Main effects plot for $NF_n$; (a) tapered angle, (b) orientation angle, and (c) $a/l$ ratio**

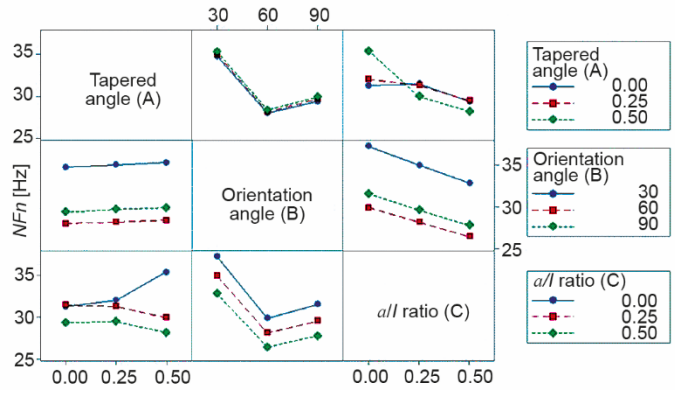


**Figure 7. Two-way interactions plot for $NF_n$**

## Regression analysis

The effects of factors main, two-way/three-way interactions, and squares on the $NF_n$ are statistically predicted with a determination coefficient of 95.63%, eq. (1), which is highly satisfactory. Furthermore, it is seen in fig. 8 that there is a good agreement between the predicted results obtained from the regression equation and the analysis results. In columns 6 and 7 of tab. 4, predicted analysis results, $P_i$, and residual value results, $R_i$, are given for each experiment obtained by the regression equation.

$$50.72 + 7.12A - 0.647B - 3.42\ C - 0.0141AxB - 24.2AxC + 0.0094BxC + \\ +0.049AxBxC - 0.02A^2 + 0.004631B^2 + 0.79C^2 \quad (1)$$

The standard error, Se($Pi$), and confidence interval (CI) values of the uncertainty analysis are respectively given in the eighth and 9th columns of tab. 4. Uncertainty analysis examines whether the average result of the confirmation tests is within the specified confidence interval and therefore the statistical evaluation made is sufficiently accurate. Calculation of CI is:

$$CI = P_i \pm t_{\alpha/2,n-(k+1)}\ Se(P_i) \quad (2)$$

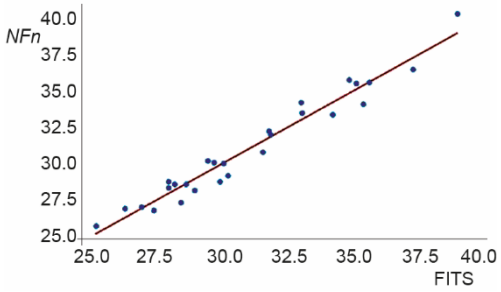


**Figure 8. Comparison of experimental and predicted responses for $NF_n$**

where $P_i$ is the predicted analysis result of the $i^{th}$ test given in sixth column of tab. 4, $\alpha$ – the significance level (0.05), $n$ – the analysis number (27), $k$ – the the number of predictors in the regression equation (10), and Se($P_i$) – the standard error of the $i^{th}$ predicted analysis. Accordingly, $t_{0,025,.16}$ is get *as* 2.12 from *t* distribution tables.

## Confirmation analyses

Four confirmation analyzes are performed at the third level of tapered angle, the first level of the orientation angle and the first level of *a/l* ratio, where the maximum $NF_n$ is obtained in the number of elements and nodes, that different from the normal analyzes, and the details of these are given in tab. 4. According to these data, average $NF_c$ of 40.149 Hz is obtained in the confirmation analyzes, and it is observed that this value is within the calculated confidence interval ($37.199 < NF_c = 40.149 < 40.448$).

**Table 4. The results of confirmation analysis**

| Confirmation analysis No. | Element number | Node number | Confirmation analysis results, $NF_c$, [Hz] |
|---|---|---|---|
| 1 | 375 | 456 | 40.031 |
| 2 | 1500 | 1661 | 40.091 |
| 3 | 3375 | 3616 | 40.205 |
| 4 | 6000 | 6321 | 40.268 |
| Average $NF_c$ = 40.149 Hz, CI = 37.199 – 40.448 | | | |

## Discussion

In this study, the natural frequency analyzes of eight layered, delaminated, and variable cross-section glass/epoxy composite beams were evaluated statistically by the Taguchi method. The highest frequency values were found to be 40.091 Hz at *a*/*l* ratio zero (no delamination), 30$^o$ orientation ratio, and 0.5 tapered angle. The reason for this is that there is no delamination in the beam, so the elasticity module of the beam remains constant and the fiber angle of the composite beam is 30$^o$ high. In addition, when the fiber angles were evaluated, it was seen that the highest frequency values were obtained at 30$^o$, then 90$^o$ was obtained at least 60$^o$. This data is supported by Zhang *et al.*, [4]. The lowest frequency values were found to be 25.699 Hz at *a*/*l* ratio of 0.5, orientation ratio 60$^o$ and tapered angle of 0.5. The reason for this is that when the delamination rate of the beam is at its maximum, the natural frequency is considered to be very low. When the cross-section angles are evaluated, 0.5 high natural frequency values are obtained, respectively, low frequency values are obtained when the cross-section angle is zero, and it can be said that the frequency increases with the increase of the tapered angle. In this investigation, the delamination is modeled in the middle of the thickness of the beam. In the future, it will be investigated how the effect of the beam on natural frequencies will change when the location of the delamination is changed. In addition, the tapered angle of the beam is modeled as linear and how the natural frequencies of the laminated composite beams will change when it comes curvilinear will be discussed.

## Conclusions

With the proposed study, the natural frequency results obtained by numerical analysis in different values of tapered angle, orientation angle, and *a*/*l* ratio in the glass/epoxy laminated composite beams are evaluated by using Taguchi experimental design method and regression analysis. Hereby, the following conclusions are obtained.

- According to ANOVA results, it is observed that all process parameters, except tapered angle-orientation angle interaction, are significant. In addition, orientation angle (68.97%) has the most significant effect on the natural frequency, and it is followed by *a*/*l* ratio (20.03%), tapered angle-*a*/*l* ratio (10.37%), tapered angle (0.31%), orientation angle- *a*/*l* ratio (0.22%) factors and interactions.
- According to the main effects plot, it is observed that the natural frequency correlates positively with tapered angle but negatively with *a*/*l* ratio, and there is a dramatic increase in the natural frequency in the orientation angle of 30°.
- The effects of factors main, two-way/three-way interactions and squares on the natural frequency are statistically predicted with a coefficient of determination of 95.63%.
- When ANOVA, main effects plot and interactions plot are taken into account, maximum natural frequency is obtained as 40.091 Hz at the third level of the tapered angle ($A$ = 0.5), the first level of the fiber angle ($B$ = 30°) and the first level of the *a*/*l* ratio ($C$ = 0). In four confirmation tests performed at these levels, an average natural frequency value of 40.149 Hz is observed. Since this value is within the calculated confidence interval, the method has achieved the optimization of the system with sufficient accuracy.
- In four validation experiments performed at these levels, an average natural frequency value of 40.149 Hz was observed. Since this value is within the calculated confidence interval, the method has performed the optimization of the system with sufficient accuracy.

- It has been showed that the natural frequency value of the beam can be changed by changing the $a/l$ ratio, tapered angle and fiber orientation angle without changing the geometry of the laminated composite beam.

## References

[1] Guo, Q., *et al.*, Constitutive Models for the Structural Analysis of Composite Materials for the Finite Element Analysis: A Review of Recent Practices, *Composite Structures, 260*, (2021), Mar., 113267
[2] Zakaria, M. R., *et al.*, Hybrid Carbon Fiber-Carbon Nanotubes Reinforced Polymer Composites: A Review, Composites Part B: *Engineering, 176* (2019), Nov., 107313
[3] Yalcın, B., Ergene, B., Analyzing the Effect of Crack in Different Hybrid Composite Materials on Mechanical Behaviors, *Pamukkale University Journal of Engineering Sciences, 24*, (2018), 4, pp. 616-625
[4] Zhang, Y. Y., *et al.*, Assessment of Timoshenko Beam Models for Vibrational Behavior of Single-Walled Carbon Nanotubes Using Molecular Dynamics, *Advances in Applied Mathematics and Mechanics, 1* (2009), 1, pp. 89-106
[5] Wang, C. Y., Influence of Gravity and Taper on the Vibration of a Standing Column, *Advances in Applied Mathematics and Mechanics, 4* (2012), June, pp. 483-495
[6] Imran, M., *et al.*, Investigating the Effect of Delamination Size, Stacking Sequences and Boundary Conditions on the Vibration Properties of Carbon Fiber Reinforced Polymer Composite, *Materials Research, 22* (2019), 2, pp. 1-7
[7] Wang, Y. J., *et al.*, Free Vibration Analysis of Composite Sandwich Panels with Hierarchical Honeycomb Sandwich Core, *Thin-Walled Structures, 145* (2019), Dec., 106425
[8] Hosseini, S., *et al.*, Characterization of the Guided Wave Propagation in Simplified Foam, Honeycomb And Hollow Sphere Structures , Composites Part B: *Engineering, 56* (2014), Jan., pp. 553-566
[9] Sayyad, A., Ghugal, Y., Bending, Buckling and Free Vibration of Laminated Composite and Sandwich Beams: A Critical Review of Literature, *Composite Structures, 171* (2017), July, pp. 486-504
[10] Ramtekkar, G. S., Free Vibration Analysis of Delaminated Beams using Mixed Finite Element Model , *Journal of Sound and Vibration, 328* (2009), 4-5, pp. 428-440
[11] Alnefaie, K., Finite Element Modeling of Composite Plates with Internal Delamination, *Composite Structures, 90* (2009), 1, pp. 21-27
[12] Della, C. N., Shu, D., Free Vibration Analysis of Multiple Delaminated Beams under Axial Compressive Load, *Journal of Reinforced Plastics and Composites, 28* (2009), 11, pp. 1365-1380
[13] Zhang, Z., *et al.*, Modal Characteristics of Micro-Perforated Sandwich Beams with Square Honeycomb-Corrugation Hybrid Cores: A Mixed Experimental-Numerical Study, *Thin-Walled Structures, 137* (2019), Apr., pp. 185-196
[14] Wang, Y., *et al.*, Free Vibration Analysis of Composite Sandwich Panels with Hierarchical Honeycomb Sandwich Core, *Thin-Walled Structures, 145* (2019), Dec., 106425
[15] Atlıhan, G., *et al.*, Free Vibration and Buckling Analysis of the Laminated Composite Beams by Using GDQM, *Advanced Composites Letters, 18* (2009), 2, pp. 37-44
[16] *** ANSYS 10.0 User's Manual, (2005)
[17] Atlıhan, G., Ergene, B., Vibration Analysis of Layered Composite Beam with Variable Section in Terms of Delamination and Orientation Angle in Analytical and Numerical Methods, *Acta Physica Polonica A, 134* (2018), 1, pp. 13-17
[18] Callıoglu, H., *et al.*, Vibration Analysis of Multiple Delaminated Composite Beams, *Advanced Composite Materials, 21* (2012), 1, pp. 11-27
[19] Ramalinggeswara, S. R., Ganesan, N., Dynamic Response of Tapered Composite Beams Using Higher Order Shear Deformation Theory, *Journal of Sound and Vibration, 187* (1995), 5, pp. 737-756
[20] Shridhar Phadke, M., *Quality Engineering Using Robust Design*, Prentice Hall, Upper Saddle. River, N. J., USA, 1989
[21] Unal, R., Dean, E. B., Taguchi Approach to Design Optimization for Quality and Cost: An overview, *Proceedings*, 13th Annual Conference of the International Society of Parametric Estimators, New Orleans. La., USA,1991
[22] Phillip Ross, J., *Taguchi Technique for Quality Engineering*, McGraw-Hill, New York, USA, 1998
[23] Pinar, A. M., Optimization of Process Parameters with Minimum Surface Roughness in the Pocket Machining of AA5083 Aluminum Alloy via Taguchi Method, *The Arabian Journal for Science and Engineering B: Engineering, 38* (2013), Oct., pp. 705-714

[24] Pinar, A. M., *et al.,* A Comparison of Cooling Methods in the Pocket Milling of AA5083-H36, *The International Journal of Advanced Manufacturing Technology, 83* (2016), Aug., pp. 1431-1440
[25] Pinar, A. M., Fırat, H., Machinability Evaluation of Multi-Directional Turning Tools, *Materials Testing, 62* (2020), Feb., pp. 311-316

Paper submitted: December 30, 2022
Paper revised: February 5, 2023
Paper accepted: March 11, 2023